mathematics

MDPI

Article

A Parallel-Viscosity-Type Subgradient Extragradient-Line Method for Finding the Common Solution of Variational Inequality Problems Applied to Image Restoration Problems

Suthep Suantai [1], Pronpat Peeyada [2] and Damrongsak Yambangwai [2,*] and Watcharaporn Cholamjiak [2]

[1] Research Center in Mathematics and Applied Mathematics, Department of Mathematics, Faculty of Science, Chiang Mai University, Chiang Mai 50200, Thailand; suthep.s@cmu.ac.th
[2] School of Science, University of Phayao, Phayao 56000, Thailand; pronpat.pee@gmail.com (P.P.); c-wchp007@hotmail.com (W.C.)
* Correspondence: damrongsak.ya@up.ac.th

Received: 8 January 2020; Accepted: 9 February 2020; Published: 14 February 2020

Abstract: In this paper, we study a modified viscosity type subgradient extragradient-line method with a parallel monotone hybrid algorithm for approximating a common solution of variational inequality problems. Under suitable conditions in Hilbert spaces, the strong convergence theorem of the proposed algorithm to such a common solution is proved. We then give numerical examples in both finite and infinite dimensional spaces to justify our main theorem. Finally, we can show that our proposed algorithm is flexible and has good quality for use with common types of blur effects in image recovery.

Keywords: variational inequality problems; viscosity-type subgradient extragradient-line method; monotone mapping; Hilbert space

1. Introduction

Let H be a real Hilbert space with the inner product $\langle .,. \rangle$ and the induced norm $\|.\|$. Let C be a nonempty closed and convex subset of H. A mapping $f : C \to C$ is said to be a *strict contraction* if there exists $k \in [0, 1)$ such that

$$\|fx - fy\| \leq k\|x - y\|, \forall x, y \in C. \tag{1}$$

A mapping $A : C \to H$ is said to be

1. *Monotone* if

$$\langle Ax - Ay, x - y \rangle \geq 0 \text{ for all } x, y \in C; \tag{2}$$

2. *Pseudo-monotone* if

$$\langle Ay, x - y \rangle \geq 0 \Rightarrow \langle Ax, x - y \rangle \geq 0 \text{ for all } x, y \in C; \tag{3}$$

3. *L-Lipschitz continuous* if there exists a positive constant L such that

$$\|Ax - Ay\| \leq L\|x - y\| \text{ for all } x, y \in C. \tag{4}$$

In this paper, we study the following variational inequality problem (VIP) for the operator A to find $x^*, \in C$ such that

$$\langle Ax^*, y - x^* \rangle \geq 0, \forall y \in C. \tag{5}$$

The set of solutions of VIP (5) is denoted by VI(A,C). The VIP was introduced and studied by Hartman and Stampacchia in 1966 [1]. The variational inequality theory is an important tool based on studying a wide class of problems—unilateral and equilibrium problems arising in structural analysis, economics, optimization, operations research, and engineering sciences (see [2–7] and the references therein). Several algorithms have been improved for solving variational inequality and related optimization problems (see [6,8–15] and the references therein). It is well known that x is the solution of the VIP (5) if and only if x is the fixed point of the mapping $P_C(I - rA)$, $r > 0$ (see [4] for details)

$$x = P_C(x - \gamma Ax), \gamma > 0 \text{ and } r_\gamma(x) := x - P_C(x - \gamma Ax) = 0.$$

Therefore, we can find the fixed point of the mapping $P_C(I - rA)$ replaces finding the solution of VIP (5) (see [7,9]). For solving VIP (5), the projection on closed and convex sets have been used. The gradient method is the simplest projection method, in which only one projection on the feasible set needs to be computed. However, strongly monotone or inverse strongly monotone operators have been required to obtain the convergence result. In 1976, Korpelevich [16] proposed another projection method called the extragradient method for finding a saddle point, and then it was extended to finding a solution of VIP for Lipschitz continuous and monotone (even pseudomonotone) mappings A. The extragradient method is designed as follows:

$$\begin{cases} y_n = P_C(x_n - \lambda A(x_n)), \\ x_{n+1} = P_C(x_n - \lambda A(y_n)), \end{cases} \tag{6}$$

where P_C is the metric projection onto C and λ is a suitable parameter. When the structure of C is simple, the extragradient method is computable and very useful because the projection onto C can be found easily. However, the computation of a projection onto a closed convex subset is generally difficult, and two distance optimization problems in the extragradient method are solved to obtain the next approximation x_{n+1} over each iteration. This can be precious and seriously affect the efficiency of the used method. In 2011, the subgradient extragradient method was proposed in [17] for solving VIPs in Hilbert spaces. A projection onto a closed convex subset is reduced into one step and a special half-space is constructed for the projection in the second step. The method is generated as follows:

$$\begin{cases} y_n = P_C(x_n - \lambda A(x_n)), \\ x_{n+1} = P_{T_n}(x_n - \lambda A(y_n)), \end{cases} \tag{7}$$

where T_n is a half-space whose bounding hyperplane is supported on C at y_n, that is,

$$T_n = \{v \in H : \langle (x_n - \lambda A(x_n)) - y_n, v - y_n \rangle\}.$$

The authors in [17] proved that two sequences $\{x_n\}, \{y_n\}$ generated by (7) converge weakly to a solution of the VIP.

Recently, Gibali [18] proposed a new subgradient extragradient method by using adopting Armijo-like searches, called the self-adaptive subgradient extragradient method. Under the assumption of pseudomonotonicity and continuity of the operator, it has been proven that the convergence result for VIP (5) is $\mathbb{R}^n$. Gibali [9] remarked that the Armijo-like searches can be viewed as a local approximation of the Lipschitz constant of A.

$$\begin{cases} x_0 \in \mathbb{R}^n, \\ y_n = P_C(x_n - \alpha A(x_n)), \ \ \alpha \in \{\alpha_{n-1}, \alpha_{n-1}\beta, \alpha_{n-1}\beta^2, ...\}, \\ (\alpha \ \text{ satisfies } \ \alpha\langle x_n - y_n, A(x_n) - A(y_n)\rangle \leq (1-\varepsilon)\|x_n - y_n\|^2), \\ x_{n+1} = P_{T_n}(x_n - \alpha_n A(y_n)), \ \ n \geq 1, \end{cases} \tag{8}$$

where $T_n = \{w \in \mathbb{R}^n \mid \langle x_n - \alpha_n A(x_n) - y_n, w - y_n\rangle \leq 0\}$, $\alpha_1 \in (0, \infty)$, and $\varepsilon, \beta \in (0,1)$.

Very recently, solving the VIP (5) when A is a Lipschitz continuous monotone mapping such that the Lipschitz constant is unknown in Hilbert spaces by using the following viscosity-type subgradient extragradient-like method was proposed by Shehu and Iyiola [19].

$$\begin{cases} y_n = P_C(x_n - \lambda_n A x_n), \ \ \lambda_n = \rho^{l_n}, \\ (l_n \text{ is the smallest non-negative integer } l \text{ such that } \lambda_n \|Ax_n - Ay_n\| \leq \mu \|r_{\rho^{l_n}}(x_n)\|), \\ z_n = P_{T_n}(x_n - \lambda_n Ayn), \\ x_{n+1} = \alpha_n f(x_n) + (1-\alpha_n) z_n, \ \ n \geq 1, \end{cases} \tag{9}$$

where $T_n = \{z \in H : \langle x_n - \lambda_n A x_n - y_n, z - y_n\rangle \leq 0\}$ with $\rho, \mu \in (0,1)$ and $\{\alpha_n\} \subseteq (0,1)$. It was proved that the sequence $\{x_n\}$ generated by (9) converges strongly to $x^* \in$ VI(C,A), where $x^* = P_{VI(C,A)} f(x^*)$ is the unique solution of the variational inequality

$$\langle (I - f)x^*, x - x^* \rangle \geq 0, \forall x \in VI(C, A), \tag{10}$$

where $f : H \to H$ is a strict contraction mapping such that constant $k \in [0,1)$ under the following conditions:

$$(C_1) \ \lim_{n\to\infty} \alpha_n = 0 \ \text{ and } \ (C_2) \ \sum_{n=1}^{\infty} \alpha_n = \infty.$$

Our interest in this paper is to study the finding of common solutions of variational inequality problems (CSVIPs). The CSVIP is stated as follows: Let C be a nonempty closed and convex subset of H. Let $A_i : H \to H, \ i = 1, 2, ..., N$ be mappings. The CSVIP is to find $x^* \in C$ such that

$$\langle A_i x^*, x - x^* \rangle \geq 0, \ \forall x \in C, \ i = 1, 2, ..., N. \tag{11}$$

If $N = 1$, CSVIP (11) becomes VIP (5).

The CSVIP has received a great deal of attention due to its applications in a large variety of problems arising in structural analysis, convex feasibility problems, common fixed point problems, common minimizer problems, common saddle-point problems, and common variational inequality problems [20]. These problems have practical applicabilities in signal processing, network resource allocation, image processing, and many other fields [21,22]. Recently, many mathematicians have been widely studying this problem both theoretically and algorithmically; see [23–27] and the references therein.

Very recently, Anh and Hieu [28,29] proposed an important method for finding a common fixed point of a finite family of quasi $\emptyset$-nonexpansive mappings $\{S_i\}_{i=1}^N$ in Banach spaces, which they called the parallel monotone hybrid algorithm. This algorithm is related to Hilbert spaces as follows:

$$\begin{cases} x_0 \in C, \\ y_n^i = \alpha_n x_n + (1-\alpha_n) S_i x_n, i = 1, ..., N, \\ i_n = \text{argmax}\{\|y_n^i - x_n\| : i = 1, ..., N\}, \bar{y}_n := y_n^{i_n}, \\ C_{n+1} = \{v \in C_n : \|v - \bar{y}_n^i\| \leq \|v - x_n\|\}, \\ x_{x+1} = P_{C_{n+1}} x_0, \end{cases} \tag{12}$$

where $0 < \alpha_n < 1$, $\limsup_{n\to\infty} \alpha_n < 1$. We see that a parallel algorithm is an algorithm that can execute several directions simultaneously on different processing devices and then combine all the individual outputs.

Inspired and encouraged by the previous results, in this paper we introduce a modified parallel method with a viscosity-type subgradient extragradient-like method for finding a common solution of variational inequality problems. Numerical experiments are also conducted to illustrate the efficiency of the proposed algorithms. Moreover, the problem of multiblur effects in an image is solved by applying our proposed algorithm.

2. Preliminaries

In order to prove our main result, we recall some basic definitions and lemmas needed for further investigation. In a Hilbert space H, let C be a nonempty closed and convex subset of H. For every point $x \in H$, there exists a unique nearest point of C, denoted by $P_C x$, such that $\|x - P_C x\| \leq \|x - y\|$ for all $y \in C$. Such a P_C is called the metric projection from H onto C.

Lemma 1 ([30]). *Let C be a nonempty closed and convex subset of a real Hilbert space H and let P_C be the metric projection of H onto C. Let $x \in H$ and $z \in C$. Then, $z = P_C x$ if and only if*

$$\langle x - z, y - z\rangle \leq 0, \ \ \forall y \in C.$$

Lemma 2 ([30]). *The following statements hold in any real Hilbert space H:*

$$(i)\ \|x + y\|^2 = \|x\|^2 + 2\langle x, y\rangle + \|y\|^2, \ \forall x, y \in H.$$
$$(ii)\ \|x + y\|^2 \leq \|x\|^2 + 2\langle y, x + y\rangle, \ \forall x, y \in H.$$

Lemma 3 (Xu, [31]). *Let $\{a_n\}_{n=0}^{\infty}$ be a sequence of non-negative real numbers satisfying the following relation:*

$$a_{n+1} \leq (1 - \alpha_n)a_n + \alpha_n\sigma_n + \gamma_n, \ n \geq 1,$$

where

(i) $\{\alpha_n\}_{n=0}^{\infty} \subset [0, 1], \Sigma_{n=1}^{\infty}\alpha_n = \infty$;
(ii) $\limsup_{n\to\infty} \sigma_n \leq 0$;
(iii) $\gamma_n \geq 0\ (n \geq 1), \Sigma_{n=1}^{\infty}\gamma_n < \infty$.

Then, $a_n \to 0$ as $n \to \infty$.

Lemma 4 ([8]). *Let C be a nonempty closed and convex subset of a real Hilbert space H and $P_C : H \to C$ is the metric projection from H onto C. Then, the following inequality holds:*

$$\|x - y\|^2 \geq \|x - P_C x\|^2 + \|y - P_C x\|^2 \ \ \forall x \in H, \forall y \in C. \tag{13}$$

Lemma 5 ([19]). *There exists a nonnegative integer l_n satisfying (9).*

Lemma 6 ([32]). *For each $x_1, x_2, ..., x_m \in H$ and $\alpha_1, \alpha_2, ..., \alpha_m \in [0, 1]$ with $\sum_{i=1}^{m} \alpha_i = 1$, we have*

$$\|\alpha_1 x_1 + ... + \alpha_m x_m\|^2 = \sum_{i=1}^{m} \alpha_i \|x_i\|^2 - \sum_{1\leq i<j\leq m} \alpha_i\alpha_j\|x_i - x_j\|^2.$$

3. Main Results

In this section, we propose the parallel method with the viscosity-type subgradient extragradient-like method modified for solving common variational inequality problems. Let C be a nonempty closed and convex subset of a real Hilbert space H. Let $A_i : C \to H$ be a monotone mapping and L_i-Lipschitz continuous on H but L_i is unknown for all $i = 1, 2, ..., N$ such that $F := \bigcap_{i=1}^{N} VI(C, A_i) \neq \emptyset$. Let $f : C \to C$ be a strict contraction mapping with constant $k \in (0, 1]$. Suppose $\{x_n\}_{n=1}^{\infty}$ is generated in the following Algorithm 1:

Algorithm 1. *Given $\rho \in (0,1), \mu \in (0,1)$. Let $\{\alpha_n\}_{n=1}^{\infty}$ be a real sequence in $(0,1)$. Let $x_1 \in H$ be arbitrary.*

Step 1 : *Compute y_n^i for all $i = 1, 2, ..., N$ by*

$$y_n^i = P_C(x_n - \lambda_n^i A_i x_n), \forall_n \geq 1,$$

where $\lambda_n^i = \rho^{l_n^i}$ and l_n^i is the smallest non-negative integer l^i such that

$$\lambda_n^i \parallel A_i x_n - A_i y_n^i \parallel \leq \mu \parallel r_{\rho^{l^i}}(x_n) \parallel . \tag{14}$$

Step 2 : *Compute*

$$z_n^i = P_{T_n^i}(x_n - \lambda_n^i A_i y_n^i),$$

where $T_n^i := \{z \in H : \langle x_n - \lambda_n^i A_i x_n - y_n^i, z - y_n^i \rangle \leq 0\}$.

Step 3 : *Compute*

$$x_{n+1} = \alpha_n^0 f(x_n) + \sum_{i=1}^{N} \alpha_n^i z_n^i, n \geq 1. \tag{15}$$

Set $n + 1 \to n$ and go to Step 1.

Theorem 1. *Assume that*

(a) $\lim_{n\to\infty} \alpha_n^0 = 0, \sum_{n=1}^{\infty} \alpha_n^0 = \infty$

(b) $\liminf_{n\to\infty} \alpha_n^i > 0, \forall_i = 1, 2, ..., N.$

Then the sequence $\{x_n\}_{n=1}^{\infty}$ generated by Algorithm 1 strongly converges to $x^* \in F$, where $x^* = P_F f(x^*)$ is the unique solution of the variational inequality:

$$\langle (I - f)x^*, x - x^* \rangle \geq 0, \forall x \in F. \tag{16}$$

Proof. Let $x^* \in F$ and $u_n^i = x_n - \lambda_n^i A_i y_n^i, \forall n \geq 1, i = 1, 2, .., N$

$$\begin{aligned} \parallel z_n^i - x^* \parallel^2 &= \langle P_{T_n^i}(u_n^i) - x^*, P_{T_n^i}(u_n^i) - x^* \rangle \\ &= \parallel P_{T_n^i}(u_n^i) - u_n^i \parallel^2 + 2\langle P_{T_n^i}(u_n^i) - u_n^i, u_n^i - x^* \rangle + \parallel u_n^i - x^* \parallel^2 \\ &= \parallel u_n^i - x^* \parallel^2 + \parallel u_n^i - P_{T_n^i}(u_n^i) \parallel^2 + 2\langle P_{T_n^i}(u_n^i) - u_n^i, u_n^i - x^* \rangle. \end{aligned} \tag{17}$$

By the characterization of the metric projection $P_{T_n}^i$ and $x^* \in F \subseteq C \subseteq T_n^i$, we get

$$2 \parallel u_n^i - P_{T_n^i}(u_n^i) \parallel^2 + 2\langle P_{T_n^i}(u_n^i) - u_n^i, u_n^i - x^* \rangle$$

$$= 2\langle u_n^i - P_{T_n^i}(u_n^i), x^* - P_{T_n^i}(u_n^i)\rangle \leq 0. \tag{18}$$

This implies that

$$\| u_n^i - P_{T_n^i}(u_n^i) \|^2 + 2\langle P_{T_n^i}(u_n^i) - u_n^i, u_n^i - x^*\rangle \leq - \| u_n^i - P_{T_n^i}(u_n^i) \|^2 . \tag{19}$$

We then obtain by the definition of Algorithm 1 that

$$\begin{aligned} \| z_n^i - x^* \|^2 &\leq \| u_n^i - x^* \|^2 - \| u_n^i - z_n^i \|^2 \\ &= \| (x_n - \lambda_n^i A_i y_n^i) - x^* \|^2 - \| (x_n - \lambda_n^i A_i y_n^i) - z_n^i \|^2 \\ &= \| x_n - x^* \|^2 - \| x_n - z_n^i \|^2 + 2\lambda_n^i \langle - x_n + x^*, A_i y_n^i\rangle \\ &\quad + 2\lambda_n^i \langle x_n - z_n^i, A_i y_n^i\rangle \\ &= \| x_n - x^* \|^2 - \| x_n - z_n^i \|^2 + 2\lambda_n^i \langle x^* - z_n^i, A_i y_n^i\rangle. \end{aligned} \tag{20}$$

By the monotonicity of the operator A_i, we have

$$\begin{aligned} 0 &\leq \langle A_i y_n^i - A_i x^*, y_n^i - x^*\rangle \\ &= \langle A_i y_n^i, y_n^i - x^*\rangle - \langle A_i x^*, y_n^i - x^*\rangle \\ &\leq \langle A_i y_n^i, y_n^i - x^*\rangle \\ &= \langle A_i y_n^i, y_n^i - z_n^i\rangle + \langle A_i y_n^i, z_n^i - x^*\rangle. \end{aligned}$$

Thus

$$\langle x^* - z_n^i, A_i y_n^i\rangle \leq \langle A_i y_n^i, y_n^i - z_n^i\rangle. \tag{21}$$

Using (20) in (21), we obtain

$$\begin{aligned} \| z_n^i - x^* \|^2 &\leq \| x_n - x^* \|^2 - \| x_n - z_n^i \|^2 + 2\lambda_n^i \langle A_i y_n^i, y_n^i - z_n^i\rangle \\ &= \| x_n - x^* \|^2 + 2\langle \lambda_n^i A_i y_n^i, y_n^i - z_n^i\rangle - 2\langle x_n - y_n^i, y_n^i - z_n^i\rangle \\ &\quad - \| x_n - y_n^i \|^2 - \| y_n^i - z_n^i \|^2 \\ &= \| x_n - x^* \|^2 + 2\langle - \lambda_n^i A_i y_n^i + x_n - y_n^i, z_n^i - y_n^i\rangle \\ &\quad - \| x_n - y_n^i \|^2 - \| y_n^i - z_n^i \|^2 \\ &= \| x_n - x^* \|^2 + 2\langle x_n - \lambda_n^i A_i y_n^i - y_n^i, z_n^i - y_n^i\rangle \\ &\quad - \| x_n - y_n^i \|^2 - \| y_n^i - z_n^i \|^2 . \end{aligned} \tag{22}$$

Observe that

$$\begin{aligned} \langle x_n - \lambda_n^i A_i y_n^i - y_n^i, z_n^i - y_n^i\rangle &= \langle x_n - \lambda_n^i A_i x_n - y_n^i, z_n^i - y_n^i\rangle + \langle \lambda_n^i A_i x_n - \lambda_n^i A_i y_n^i, z_n^i - y_n^i\rangle \\ &\leq \langle \lambda_n^i A_i x_n - \lambda_n^i A_i y_n^i, z_n^i - y_n^i\rangle. \end{aligned}$$

Using the last inequality in (22) and Lemma 5, we have

$$\begin{aligned} \| z_n^i - x^* \|^2 &\leq \| x_n - x^* \|^2 + 2\langle \lambda_n^i A_i x_n - \lambda_n^i A_i y_n^i, z_n^i - y_n^i\rangle - \| x_n - y_n^i \|^2 - \| y_n^i - z_n^i \|^2 \\ &\leq \| x_n - x^* \|^2 + 2\lambda_n^i \| A_i x_n - A_i y_n^i \| \| z_n^i - y_n^i \| - \| x_n - y_n^i \|^2 - \| y_n^i - z_n^i \|^2 \\ &\leq \| x_n - x^* \|^2 + 2\mu \| x_n - y_n^i \| \| z_n^i - y_n^i \| - \| x_n - y_n^i \|^2 - \| y_n^i - z_n^i \|^2 \\ &\leq \| x_n - x^* \|^2 + \mu(\| x_n - y_n^i \|^2 + \| z_n^i - y_n^i \|^2) - \| x_n - y_n^i \|^2 - \| y_n^i - z_n^i \|^2 \\ &= \| x_n - x^* \|^2 - (1-\mu) \| x_n - y_n^i \|^2 - (1-\mu) \| y_n^i - z_n^i \|^2 . \end{aligned} \tag{23}$$

It follows from (15) and (23) that

$$\| x_{n+1} - x^* \| = \| \alpha_n^0 f(x_n) + \sum_{i=1}^{N} \alpha_n^i z_n^i - x^* \|$$

$$
\begin{aligned}
&\leq \alpha_n^0 \parallel f(x_n) - x^* \parallel + \sum_{i=1}^{N} \alpha_n^i \parallel z_n^i - x^* \parallel \\
&\leq \alpha_n^0 \parallel f(x_n) - f(x^*) \parallel + \alpha_n^0 \parallel f(x^*) - x^* \parallel + \sum_{i=1}^{N} \alpha_n^i \parallel z_n^i - x^* \parallel \\
&\leq \alpha_n^0 k \parallel x_n - x^* \parallel + \sum_{i=1}^{N} \alpha_n^i \parallel x_n - x^* \parallel + \alpha_n^0 \parallel f(x^*) - x^* \parallel \\
&= (1 - \alpha_n^0(1-k)) \parallel x_n - x^* \parallel + \alpha_n^0 \parallel f(x^*) - x^* \parallel \\
&= (1 - \alpha_n^0(1-k)) \parallel x_n - x^* \parallel + \alpha_n^0(1-k) \tfrac{\|f(x^*) - x^*\|}{1-k} \\
&\leq \max \left\{ \parallel x_n - x^* \parallel, \tfrac{\|f(x^*) - x^*\|}{1-k} \right\} \\
&\vdots \\
&\leq \max \left\{ \parallel x_1 - x^* \parallel, \tfrac{\|f(x^*) - x^*\|}{1-k} \right\}.
\end{aligned}
$$

This implies that $\{x_n\}$ is bounded. Consequently, $\{f(x_n)\}$, $\{y_n^i\}$, and $\{z_n^i\}$ are also bounded.

Let $z = P_F f(z)$. From (15) and (23), we have

$$
\begin{aligned}
\parallel x_{n+1} - z \parallel^2 &= \parallel \alpha_n^0 f(x_n) - \sum_{i=1}^{N} \alpha_n^i z_n^i - z \parallel^2 \\
&= \parallel \alpha_n^0 (f(x_n) - z) + \sum_{i=1}^{N} \alpha_n^i (z_n^i - z) \parallel^2 \\
&\leq \alpha_n^0 \parallel f(x_n) - z \parallel^2 + \sum_{i=1}^{N} \alpha_n^i \parallel z_n^i - z \parallel^2 \\
&\leq \alpha_n \parallel f(x_n) - z \parallel^2 + \sum_{i=1}^{N} \alpha_n^i (\parallel x_n - z \parallel^2 \\
&\quad -(1-\mu) \parallel x_n - y_n^i \parallel^2 - (1-\mu) \parallel y_n^i - z_n^i \parallel^2) \\
&= \sum_{i=1}^{N} \alpha_n^i \parallel x_n - z \parallel^2 + \alpha_n^0 \parallel f(x_n) - z \parallel^2 \\
&\quad - \sum_{i=1}^{N} \alpha_n^i (1-\mu) \parallel x_n - y_n^i \parallel^2 - \sum_{i=1}^{N} \alpha_n^i (1-\mu) \parallel y_n^i - z_n^i \parallel^2 \\
&\leq \parallel x_n - z \parallel^2 + \alpha_n^0 \parallel f(x_n) - z \parallel^2 - \sum_{i=1}^{N} \alpha_n^i (1-\mu) \parallel x_n - y_n^i \parallel^2 \\
&\quad - \sum_{i=1}^{N} \alpha_n^i (1-\mu) \parallel y_n^i - z_n^i \parallel^2 .
\end{aligned} \tag{24}
$$

Furthermore, using Lemma 2 (ii) in (15), we obtain

$$\begin{aligned}
\| x_{n+1} - z \|^2 &= \| \alpha_n^0 f(x_n) + \sum_{i=1}^{N} \alpha_n^i z_n^i - z \|^2 \\
&= \| \alpha_n^0 (f(x_n) - z) + \sum_{i=1}^{N} \alpha_n^i (z_n^i - z) \|^2 \\
&= \| \sum_{i=1}^{N} \alpha_n^i (z_n^i - z) + \alpha_n^0 (f(x_n) - z) \|^2 \\
&\leq (1-\alpha_n^0)^2 \| x_n - z \|^2 + 2\alpha_n^0 \langle f(x_n) - z, x_{n+1} - z \rangle \\
&= (1-\alpha_n^0)^2 \| x_n - z \|^2 + 2\alpha_n^0 \langle f(x_n) - f(z), x_{n+1} - z \rangle \\
&\quad + 2\alpha_n^0 \langle f(z) - z, x_{n+1} - z \rangle \\
&\leq (1-\alpha_n^0)^2 \| x_n - z \|^2 + 2\alpha_n^0 k \| x_n - z \| \| x_{n+1} - z \| \\
&\quad + 2\alpha_n^0 \langle f(z) - z, x_{n+1} - z \rangle \\
&\leq (1-\alpha_n^0)^2 \| x_n - z \|^2 + \alpha_n^0 k (\| x_n - z \|^2 + \| x_{n+1} - z \|^2) \\
&\quad + 2\alpha_n^0 \langle f(z) - z, x_{n+1} - z \rangle
\end{aligned} \tag{25}$$

which implies that for some $M > 0$,

$$\begin{aligned}
\| x_{n+1} - z \|^2 &\leq \frac{(1-\alpha_n^0)^2 + \alpha_n^0 k}{1-\alpha_n^0 k} \| x_n - z \|^2 + \frac{2\alpha_n^0}{1-\alpha_n^0 k} \langle f(z) - z, x_{n+1} - z \rangle \\
&= \frac{1 - 2\alpha_n^0 + \alpha_n^0 k}{1-\alpha_n^0 k} \| x_n - z \|^2 + \frac{(\alpha_n^0)^2}{1-\alpha_n^0 k} \| x_n - z \|^2 + \frac{2\alpha_n^0}{1-\alpha_n^0 k} \langle f(z) - z, x_{n+1} - z \rangle \\
&\leq \left(1 - \frac{2(1-k)\alpha_n^0}{(1-\alpha_n^0)k}\right) \| x_n - z \|^2 + \frac{2(1-k)\alpha_n^0}{(1-\alpha_n^0)k} \\
&\quad \times \left[\frac{\alpha_n^0}{2(1-k)} \| x_n - z \|^2 + \frac{1}{1-k} \langle f(z) - z, x_{n+1} - z \rangle \right] \\
&\leq \left(1 - \frac{2(1-k)\alpha_n^0}{1-\alpha_n^0 k}\right) \| x_n - z \|^2 + \frac{2(1-k)\alpha_n^0}{1-\alpha_n^0 k} \\
&\quad \times \left[\frac{\alpha_n^0}{2(1-k)} M + \frac{1}{1-k} \langle f(z) - z, x_{n+1} - z \rangle \right].
\end{aligned} \tag{26}$$

We will divide the next proof into two parts.

Case 1 Suppose that there exists $n_0 \in \mathbb{N}$ such that $\{\| x_n - z \|\}_{n=n_0}^{\infty}$ is non-increasing. Then, $\{\| x_n - z \|\}_{n=1}^{\infty}$ converges and $\| x_n - z \|^2 - \| x_{n+1} - z \|^2 \to 0, n \to \infty$. From (24), we have

$$\sum_{i=1}^{N} \alpha_n^i (1-\mu) \| x_n - y_n^i \|^2 \leq \| x_n - z \|^2 - \| x_{n+1} - z \|^2 + \alpha_n^0 \| f(x_n) - z \|^2 . \tag{27}$$

It follows from our assumptions (i) and (ii) that

$$\lim_{n\to\infty} \| x_n - y_n^i \| = 0, \quad \forall i = 1, 2, ..., N. \tag{28}$$

Similarly, from (24), we obtain that

$$\lim_{n\to\infty} \| y_n^i - z_n^i \| = 0, \quad \forall i = 1, 2, ..., N. \tag{29}$$

Set $t_n = \alpha_n^0 x_n + \sum_{i=1}^{N} \alpha_n^i z_n^i$ and $s_n = \alpha_n^0 x_n + \sum_{i=1}^{N} \alpha_n^i y_n^i$. It follows from our assumption (i) and (29) that

$$\lim_{n\to\infty} \| x_{n+1} - t_n \| = \lim_{n\to\infty} \alpha_n^0 \| f(x_n) - x_n \| = 0 \tag{30}$$

and

$$\lim_{n\to\infty} \| t_n - s_n \| \leq \lim_{n\to\infty} \sum_{i=1}^{N} \alpha_n^i \| z_n^i - y_n^i \| = 0. \tag{31}$$

It follows from (28) that

$$\lim_{n\to\infty} \| s_n - x_n \| \leq \lim_{n\to\infty} \sum_{i=1}^{N} \alpha_n^i \| y_n^i - x_n \| = 0. \tag{32}$$

It follows from (30)–(32) that

$$\| x_{n+1} - x_n \| \leq \| x_{n+1} - t_n \| + \| t_n - s_n \| + \| s_n - x_n \| \to 0.$$

Since $\{x_n\}$ is bounded, it has a subsequence $\{x_{n_j}\}$ such that $\{x_{n_j}\}$ converges weakly to some $\omega \in H$ and $\limsup_{n\to\infty} \langle f(z) - z, x_n - z \rangle = \lim_{j\to\infty} \langle f(z) - z, x_{n_j} - z \rangle$. We show that $\omega \in F$. Now, $x_n - y_n^i \to 0$ implies that $y_{n_j}^i \rightharpoonup \omega$ and since $y_n^i \in C$, we then obtain $\omega \in C$. For all $x \in C$ and using the property of the projection P_C, we have (since A_i is monotone):

$$\begin{aligned} 0 &\leq \langle y_{n_j}^i - x_{n_j} - \lambda_{n_j}^i A_i x_{n_j}, x - y_{n_j}^i \rangle \\ &= \langle y_{n_j}^i - x_{n_j}, x - y_{n_j}^i \rangle + \lambda_n^i \langle A_i x_{n_j}, x_{n_j} - y_{n_j}^i \rangle + \lambda_{n_j}^i \langle A_i x_{n_j}, x - x_{n_j}^i \rangle \\ &\leq \langle y_{n_j}^i - x_{n_j}, x - y_{n_j}^i \rangle + \lambda_{n_j}^i \langle A_i x_{n_j}, x_{n_j} - y_{n_j}^i \rangle + \lambda_{n_j}^i \langle A_i x_{n_j}, x - x_{n_j}^i \rangle. \end{aligned}$$

Taking $j \to \infty$, we get (recall that $\inf_{n\geq 1} \lambda_{n_j} > 0$ by Remark 3.2 in [19])

$$\langle A_i \omega, x - \omega \rangle \geq 0, \quad \forall x \in C.$$

This implies that $\omega \in F$. Since $z = P_F f(z)$, we have

$$\begin{aligned} \limsup_{n\to\infty} \langle f(z) - z, x_n - z \rangle &= \lim_{j\to\infty} \langle f(z) - z, x_{n_j} - z \rangle \\ &= \langle f(z) - z, w - z \rangle \\ &\leq 0. \end{aligned}$$

Since $\lim_{n\to\infty} \| x_{n+1} - x_n \| = 0$, we have

$$\limsup_{n\to\infty} \langle f(z) - z, x_{n+1} - z \rangle \leq 0.$$

In (26), let $a_n := \| x_n - z \|^2$, $\beta_n := \frac{2(1-k)\alpha_n^0}{1-\alpha_n^0 k}$, and $\sigma_n := \frac{\alpha_n^0}{2(1-k)} M + \frac{1}{1-k} \langle f(z) - z, x_{n+1} - z \rangle$. Then, we can write (26) as

$$a_{n+1} \leq (1 - \beta_n) a_n + \beta_n \sigma_n. \tag{33}$$

It is easy to see that $\lim_{n\to\infty} \beta_n = 0$, $\sum_{n=1}^{\infty} \beta_n = \infty$, and $\limsup_{n\to\infty} \sigma_n \leq 0$.

Using Lemma 3 in (33), we obtain $\lim_{n\to\infty} \| x_n - z \| = 0$. Thus, $x_n \to z, n \to \infty$.

Case 2 Assume that $\{\| x_n - z \|\}$ is not a monotone and decreasing sequence. Set $F_n = \| x_n - z \|^2$ and let $\tau : \mathbb{N} \to \mathbb{N}$ be a mapping defined for all $n \geq n_0$ (for some n_0 large enough) by

$$\tau_{(n)} := \max \{k \in \mathbb{N} : k \leq n, F_k \leq F_{k+1}\}.$$

It is clear that τ is a non-decreasing sequence such that $\tau_{(n)} \to \infty$ as $n \to \infty$ and

$$0 \leq F_{\tau(n)} \leq F_{\tau_(n)+1}, \quad \forall n \geq n_0.$$

This implies that $\| x_{\tau(n)} - z \| \leq \| x_{\tau(n)+1} - z \|, \forall_n \geq n_0$. Thus, $\lim_{n\to\infty} \| x_{\tau(n)} - z \|$ exists. By (27), we obtain

$$\sum_{i=1}^{N} \alpha^i_{\tau(n)}(1-\mu) \| x_{\tau(n)} - y^i_{\tau(n)} \|^2 \leq \| x_{\tau(n)} - z \|^2 - \| x_{\tau(n)+1} - z \|^2 + \alpha^0_{\tau(n)} \| f(x_{\tau(n)}) - z \|^2 \to 0,$$

as $n \to \infty$. Thus,

$$\| x_{\tau(n)} - y^i_{\tau(n)} \| \to 0$$

as $n \to \infty$. As in Case 1, we can prove that

$$\lim_{n\to\infty} \| y^i_{\tau(n)} - z^i_{\tau(n)} \| = \lim_{n\to\infty} \| x_{\tau(n)+1} - z^i_{\tau(n)} \| = \lim_{n\to\infty} \| x_{\tau(n)+1} - x_{\tau(n)} \| = 0.$$

Since $\{x_{\tau(n)}\}$ is bounded, there exists a subsequence of $\{x_{\tau(n)}\}$ that converges weakly to ω. Without loss of generality, we assume that $x_{\tau(n)} \rightharpoonup \omega$. Observe that since $\lim_{n\to\infty} \| x_{\tau(n)} - y^i_{\tau(n)} \| = 0$ we also have $y^i_{\tau(n)} \rightharpoonup \omega$. By similar argument in Case 1, we can show that $\omega \in F$ and

$$\limsup_{n\to\infty} \langle f(z) - z, x_{\tau(n)} - z \rangle \leq 0.$$

Observe that since $\lim_{n\to\infty} \| x_{\tau(n)+1} - x_{\tau(n)} \| = 0$ and $\limsup_{n\to\infty} \langle f(z) - z, x_{\tau(n)} - z \rangle \leq 0$, this implies that

$$\limsup_{n\to\infty} \langle f(z) - z, x_{\tau(n)+1} - z \rangle \leq 0.$$

By (26), we obtain that

$$\begin{aligned} \| x_{\tau(n)+1} - z \|^2 &\leq \left(1 - \frac{2(1-\tau)\alpha^0_{\tau(n)}}{1-\alpha^0_{\tau(n)}k}\right) \| x_{\tau(n)} - z \|^2 + \frac{2(1-k)\alpha^0_{\tau(n)}}{1-\alpha^0_n k} \\ &\quad \times \left[\frac{\alpha^0_{\tau(n)}}{2(1-k)} M + \frac{1}{1-k}\langle f(z) - z, x_{\tau(n)+1} - z \rangle\right] \\ &= (1-\beta_{\tau(n)}) \| x_{\tau(n)} - z \|^2 + \beta_{\tau(n)} \left(\frac{\alpha^0_{\tau(n)}}{2(1-k)} M + \frac{1}{1-k}\langle f(z) - z, \right. \\ &\quad \left. x_{\tau(n)+1} - z \rangle \right) \end{aligned}$$

where $\beta_{\tau(n)} := \frac{2(1-k)\alpha^0_{\tau(n)}}{1-\alpha^0_{\tau(n)}k}$. Hence, we have (since $F_{\tau(n)} \leq F_{\tau(n)+1}$)

$$\begin{aligned} \beta_{\tau(n)} \| x_{\tau(n)} - z \|^2 &\leq \| x_{\tau(n)} - z \|^2 - \| x_{\tau(n)+1} - z \|^2 \\ &\quad + \beta_{\tau(n)} \left(\frac{\alpha^0_{\tau(n)}}{2(1-k)} M + \frac{1}{1-k}\langle f(z) - z, x_{\tau(n)+1} - z \rangle \right) \\ &\leq \beta_{\tau(n)} \left(\frac{\alpha^0_{\tau(n)}}{2(1-k)} M + \frac{1}{1-k}\langle f(z) - z, x_{\tau(n)+1} - z \rangle \right). \end{aligned}$$

Since $\alpha^0_{\tau(n)} > 0$ and $k \in [0,1)$, we have that $\beta_{\tau(n)} > 0$. So, we get

$$\| x_{\tau(n)} - z \|^2 \leq \frac{\alpha^0_{\tau(n)}}{2(1-\tau)} M + \frac{1}{1-k}\langle f(z) - z, x_{\tau(n)+1} - z \rangle,$$

and this implies that

$$\limsup_{n\to\infty} \| x_{\tau(n)} - z \|^2 \leq \limsup_{n\to\infty} \frac{\alpha^0_{\tau(n)}}{2(1-\tau)} M + \frac{1}{1-k}\langle f(z) - z, x_{\tau(n)+1} - z \rangle \leq 0.$$

Therefore,

$$\lim_{n\to\infty} \| x_{\tau(n)} - z \| = 0$$

and

$$\lim_{n\to\infty} \| x_{\tau(n)+1} - z \| = 0.$$

Hence,

$$\lim_{n\to\infty} F_{\tau(n)} = \lim_{n\to\infty} F_{\tau(n)+1} = 0.$$

Furthermore, for $n \geq n_0$, it is easy to see that $F_{\tau(n)} \leq F_{\tau(n)+1}$ if $n \neq \tau(n)$ (that is $\tau(n) < n$), because $F_j \geq F_{j+1}$ for $\tau(n)+1 \leq j \leq n$. As a consequence, we obtain for all $n \geq n_0$,

$$0 \leq F_n \leq \max\{F_{\tau(n)}, F_{\tau(n)+1}\} = F_{\tau(n)+1}.$$

Hence, $\lim F_n = 0$, that is , $\lim_{n\to\infty} \| x_n - z \| = 0$. Hence, $\{x_n\}$ converges strongly to z.

This completes the proof. □

We now give an example in Euclidian space $\mathbb{R}^3$ where $\|.\|$ is ℓ_2-norm defined by $\|x\| = \sqrt{x_1^2 + x_2^2 + x_3^2}$ where $x = (x_1, x_2, x_3)$ to support the main theorem.

Example 1. *Let* $A_1, A_2, A_3 : \mathbb{R}^3 \to \mathbb{R}^3$ *be defined by* $A_1x = 4x$, $A_2x = 7x + (5, -2, 1)$ *and* $A_3x = \begin{pmatrix} 10 & -5 & 5 \\ -5 & 10 & -5 \\ 5 & -5 & 10 \end{pmatrix} + (4, 2, 1)$ *for all* $x = (x_1, x_2, x_3)$. *Let* $f : \mathbb{R}^3 \to \mathbb{R}^3$ *be defined by* $f(x) = \frac{x}{2}$ *for all* $x \in \mathbb{R}^3$. *Let* $C = \{x \in \mathbb{R}^3 | \|x\|^2 \leq 4\}$. *We can choose* $\alpha_n^0 = \frac{1}{(n+1)^{0.3}}$, $\alpha_n^1 = \frac{1}{2n}$, $\alpha_n^2 = \frac{n}{n+1}$ *and* $\alpha_n^3 = 1 - \alpha_n^0 - \alpha_n^1 - \alpha_n^2$. *The stopping criterion is defined by* $\|x_n - x_{n-1}\| < 10^{-15}$ *(See in Figures 1–3). The different choices of* x_1 *are given in Table 1 as follows in Example 1.*

Table 1. Comparison of the number of iterations in Example 1.

Inputting	$x_1 = (-3, -5, 8)$		$x_1 = (-1, 7, 6)$		$x_1 = (6.13, -5.24, -1.19)$	
	CPU Time	**Iter No.**	**CPU Time**	**Iter No.**	**CPU Time**	**Iter No.**
A_1	0.0000068	592	0.0000056	591	0.00001	589
A_2	0.0003795	230	0.0002848	230	0.0002887	229
A_3	0.0004619	230	0.0007852	230	0.000766	229
A_1, A_2	0.0002942	231	0.0002965	231	0.0002945	231
A_1, A_3	0.0008444	231	0.0009953	231	0.0009992	231
A_2, A_3	0.0011516	230	0.0009781	230	0.0007956	229
A_1, A_2, A_3	0.0007429	231	0.0007586	231	0.0007621	231

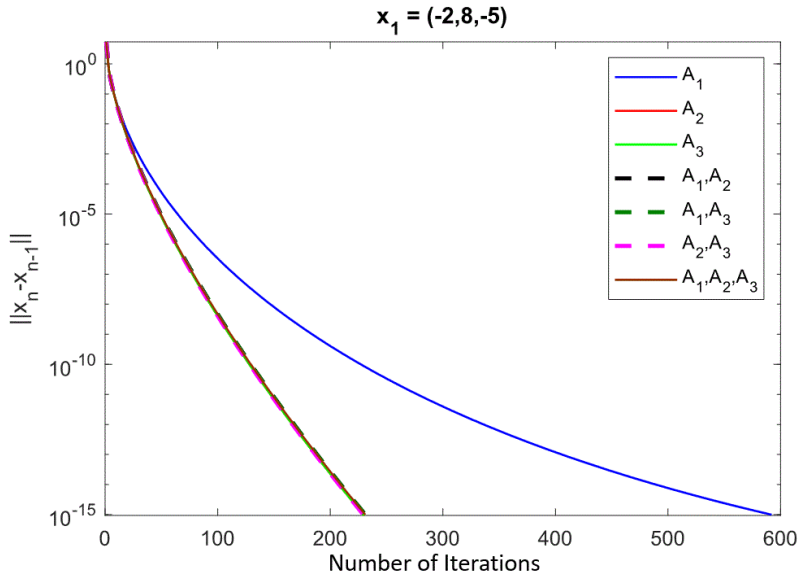

Figure 1. The error plotting $\|x_n - x_{n-1}\|$ for choice 1 in Example 1.

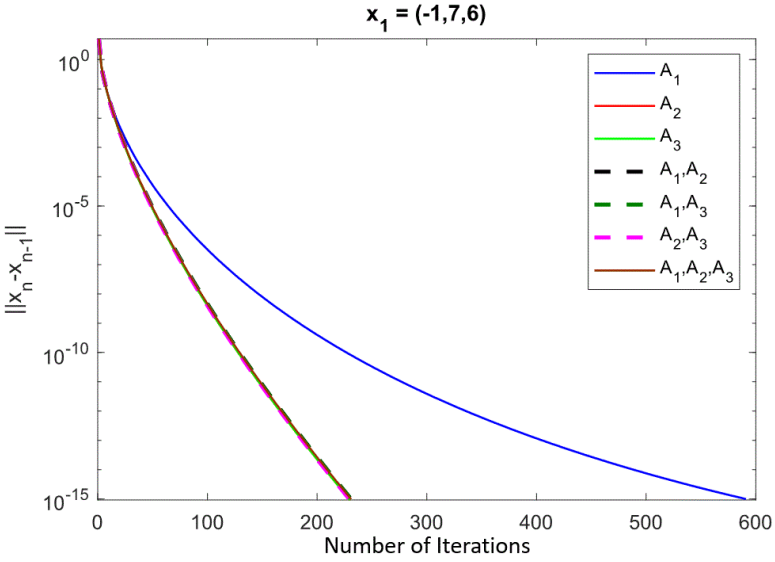

Figure 2. The error plotting $\|x_n - x_{n-1}\|$ for choice 2 in Example 1.

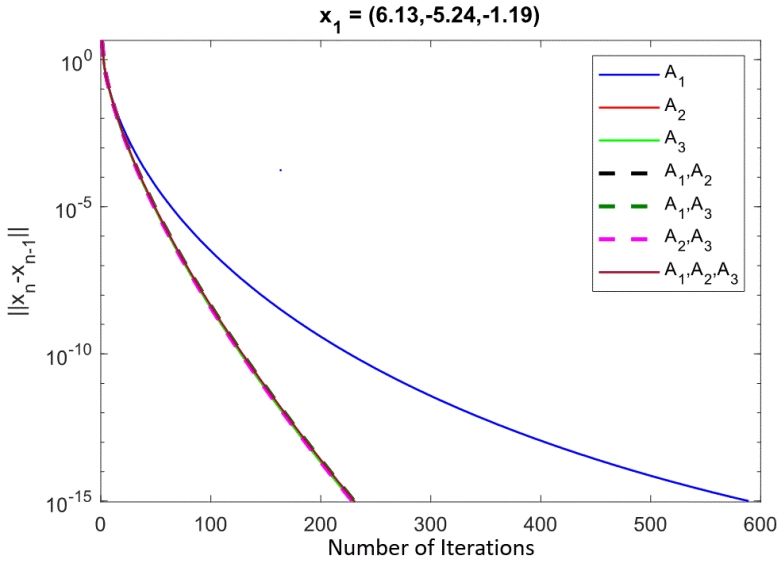

Figure 3. The error plotting $\|x_n - x_{n-1}\|$ for choice 3 in Example 1.

For infinitely dimensional space, we give an example in function space $L_2[0,1]$ such that $\|.\|$ is L_2-norm defined by $\|x(t)\| = \sqrt{\int_0^1 |x(t)|^2 dt}$ where $x(t) \in L_2[0,1]$.

Example 2. *Let $A_1, A_2, A_3 : L_2[0,1] \to L_2[0,1]$ be defined by $A_1x(t) = \int_0^t 4x(s)ds$, $A_2x(t) = \int_0^t tx(s)ds$ and $A_3x(t) = \int_0^t (t^2-1)x(s)ds$ where $x(t) \in L_2[0,1]$. Let $f : L_2[0,1] \to L_2[0,1]$ be defined by $f(x(t)) = \frac{x(t)}{2}$ where $x(t) \in L_2[0,1]$. Let $C = \{x(t) \in L_2[0,1] : \int_0^1 (t^2+1)x(t)dt\}$. We can choose $\alpha_n^0 = \frac{1}{(n+1)^{0.3}}$, $\alpha_n^1 = \frac{1}{2n}$, $\alpha_n^2 = \frac{n}{n+1}$ and $\alpha_n^3 = 1 - \alpha_n^0 - \alpha_n^1 - \alpha_n^2$. The stopping criterion is defined by $\|x_n(t) - x_{n-1}(t)\| < 10^{-5}$ (See in Figures 4–6).*

The different choices of $x_1(t)$ are given in Table 2 as follows:

Choice 1 *Bernstein initial data:* $x_1(t) = -120t^7(t-1)^3$;
Choice 2 *Chebyshev initial data:* $x_1(t) = 64t^7 - 112t^5 + 56t^3 - 7t$;
Choice 3 *Legendre initial data:* $x_1(t) = \frac{315}{128}t - \frac{1155}{32}t^3 + \frac{9009}{64}t^5 - \frac{6435}{32}t^7 + \frac{12155}{128}t^9$.

From Tables 1 and 2, we see that the advantage of the parallel viscosity type subgradient extragradient-line method Algorithm 1 when the common solution of two or more inputting A_i gives the number of iterations smaller than one inputting.

Table 2. Comparison of the number of iterations in Example 2.

Inputting	Bernstein Initial Data		Chebyshev Initial Data		Legendre Initial Data	
	CPU Time	Iter. No.	CPU Time	Iter. No.	CPU Time	Iter. No.
A_1	2.20542	40	4.53568	40	2.66656	33
A_2	2.93440	35	1.53655	39	1.46195	33
A_3	2.699356	28	2.13809	38	1.38359	32
A_1, A_2	20.5162	36	33.9656	39	20.3007	33
A_1, A_3	11.0109	29	77.1907	38	44.6389	32
A_2, A_3	7.47927	28	52.5607	38	30.7733	32
A_1, A_2, A_3	6.20955	28	82.3549	38	45.8789	32

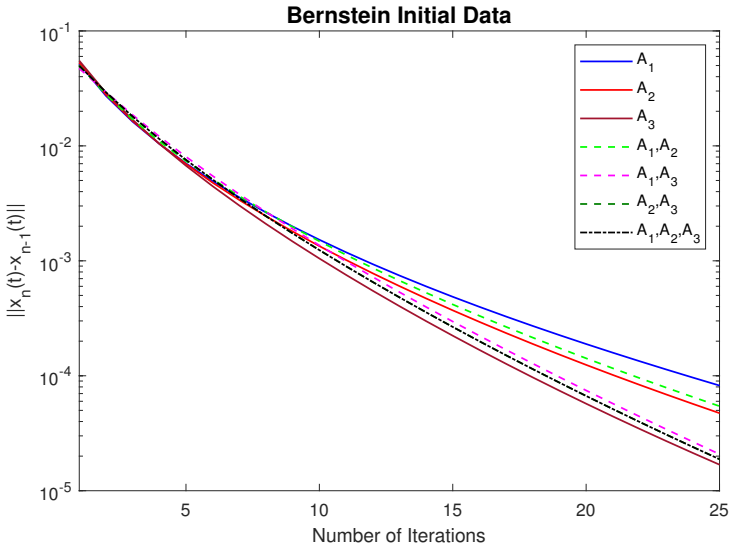

Figure 4. The error plotting $\|x_n(t) - x_{n-1}(t)\|$ for choice 1 in Example 2.

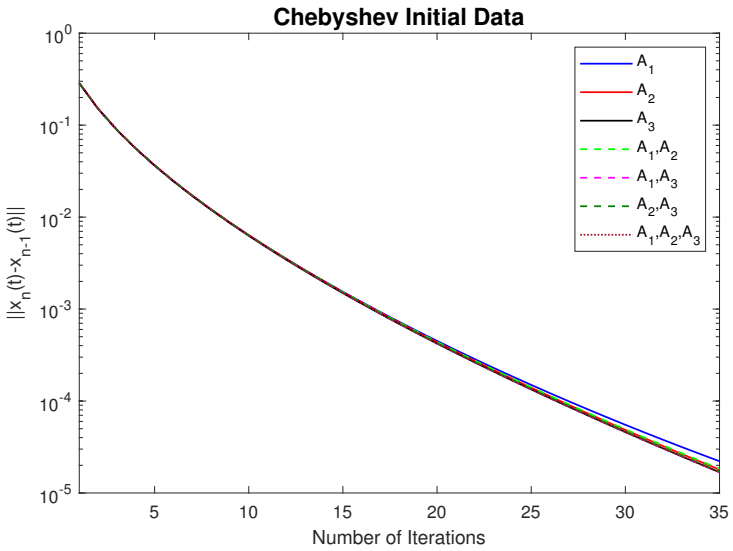

Figure 5. The error plotting $\|x_n(t) - x_{n-1}(t)\|$ for choice 2 in Example 2.

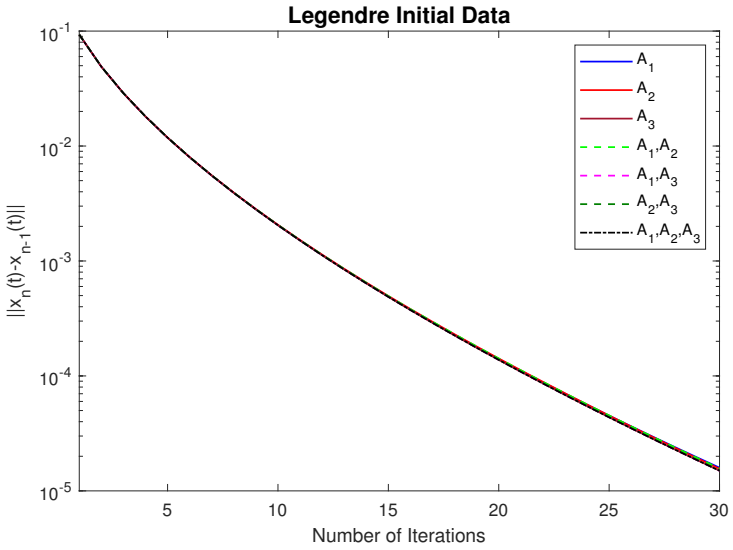

Figure 6. The error plotting $\|x_n(t) - x_{n-1}(t)\|$ for choice 3 in Example 2.

4. Application to Image Restoration Problems

The image restoration problem can be modeled in one-dimensional vectors by the following linear equation system:

$$b = Ax + v, \tag{34}$$

where $x \in \mathbb{R}^{n\times 1}$ is an original image, $b \in \mathbb{R}^{m\times 1}$ is the observed image, v is additive noise, and $A \in \mathbb{R}^{m\times n}$ is the blurring matrix. For solving problem (34), we aim to approximate the original image, vector x, by minimizing the additive noise, which is called a least squares (LS) problem as follows:

$$\min_x \frac{1}{2}\|b - Ax\|^2, \tag{35}$$

where $\|.\|$ is ℓ_2-norm defined by $\|x\| = \sqrt{\sum_{i=1}^{n} |x_i|^2}$. The solution of the problem (35) can be approximated by many well-known iteration methods.

The Richardson iteration, which is often called the Landweber method [33–36], is generally used as an iterative regularization method to solve (35). The basic iteration takes the form:

$$x_{n+1} = x_n + \tau A^T(b - Ax_n). \tag{36}$$

Here the step size τ remains constant for each iteration. The convergence can be proved under the step size τ such that $0 < \tau < \frac{2}{\sigma^2_{\max}}$ where σ_{max} is the largest singular value of A.

The goal in image restoration is to deblur an image without knowing which one is the blurring operator. Thus, we focus on the following problem:

$$\min_{x\in\mathbb{R}^n} \frac{1}{2}\|A_1x - b_1\|^2, \min_{x\in\mathbb{R}^n} \frac{1}{2}\|A_2x - b_2\|^2, ..., \min_{x\in\mathbb{R}^n} \frac{1}{2}\|A_Nx - b_N\|^2 \tag{37}$$

where x is the original true image, A_i is the blurred matrix, b_i is the blurred image by the blurred matrix A_i for all $i = 1, 2, ..., N$. For solving this problem, we designed the following flowchart:

Where $\tilde{X}$ is the deblurred image or the common solutions of the problem (37) and as seen in Figure 7. We can apply the algorithm in Theorem 1 to solve the problem (37), and as a result, we know that $A_i^T(A_ix - b_i)$ is Lipschitz continuous for each $i = 1, 2, ..., N$. Let $f : \mathbb{R}^n \to \mathbb{R}^n$ be a strict contraction

mapping with constant $k \in (0,1]$. Suppose $\{x_n\}_{n=1}^{\infty}$ is generated in the following Algorithm 2:

Algorithm 2. *Given $\rho \in (0,1)$, $\mu \in (0,1)$. Let $\{\alpha_n\}_{n=1}^{\infty}$ be a real sequence in $(0,1)$. Let $x_1 \in H$ be arbitrary.*

Step 1 : *Compute for all $i = 1, 2, ..., N$ by*

$$y_n^i = P_C(x_n - \lambda_n^i A_i^T(A_i x_n - b_i)), \forall_n \geq 1,$$

where $\lambda_n^i = \rho^{l_n^i}$ and l_n^i is the smallest nonnegative integer l^i such that

$$\lambda_n^i \parallel A_i x_n - A_i y_n^i \parallel \leq \mu \parallel r_{\rho^{l^i}}(x_n) \parallel . \tag{38}$$

Step 2 : *Compute*

$$z_n^i = P_{T_n^i}(x_n - \lambda_n^i A_i^T(A_i y_n^i - b_i)),$$

where $T_n^i := \{z \in H : \langle x_n - \lambda_n^i A_i x_n - y_n^i, z - y_n^i \rangle \leq 0\}$.

Step 3 : *Compute*

$$x_{n+1} = \alpha_n^0 f(x_n) + \sum_{i=1}^{N} \alpha_n^i z_n^i, n \geq 1. \tag{39}$$

Set $n+1 \to n$ and go to Step 1.

We will present restoration of images corrupted by the following blur types:

(1) Gaussian blur of filter size 9×9 with standard deviation $\sigma = 4$ (the original image was degraded by the blurring matrix A_1).
(2) Out-of-focus blur (disk) with radius $r = 6$ (the original image was degraded by the blurring matrix A_2).
(3) Motion blur specifying with motion length of 21 pixels (len $= 21$) and motion orientation 11° ($\theta = 11$) (the original image was degraded by the blurring matrix A_3).

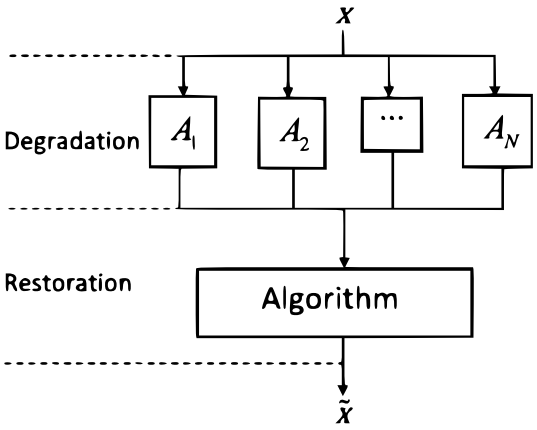

Figure 7. The flowchart of the image restoration process.

The performance of the studied proposed Algorithm 2 with the following original grey and RGB images was tested, as can be seen in Figures 8 and 9.

Figure 8. The matrix size of grey image is 276×490.

Figure 9. The matrix size of RGB image is $280 \times 497 \times 3$.

The parameter α_n^i on the implemented algorithm for solving the problem (VIP) was set as

$$\alpha_n^i = \frac{n}{n+1}, \ i = 1, 2, 3.$$

Three different types of blurred grey and RGB images degraded by the blurring matrices A_1, A_2 and A_3 are shown in Figures 10–15.

Figure 10. Three degraded grey image by blurred matrices A_1, A_2, and A_3, respectively.

Out of Focus Blurred Image with radius = 6

Figure 11. Three degraded grey image by blurred matrices A_1, A_2, and A_3, respectively.

Motion Blurred Image with len = 21 and θ =11

Figure 12. Three degraded grey image by blurred matrices A_1, A_2, and A_3, respectively.

Gaussian Blurred Image with hsize = [9x9] and σ = 4

Figure 13. Three degraded RGB image by blurred matrices A_1, A_2, and A_3, respectively.

Figure 14. Three degraded RGB image by blurred matrices A_1, A_2, and A_3, respectively.

Figure 15. Three degraded RGB image by blurred matrices A_1, A_2, and A_3, respectively.

We applied the proposed algorithm to obtain the solution of the deblurring problem (VIP) with ($N = 1$) by inputting A_1, A_2, and A_3. The results of the proposed algorithm with 10,000 iterations for the following three cases:

Case I: Inputting A_1 in the proposed algorithm;
Case II: Inputting A_2 in the proposed algorithm; and
Case III: Inputting A_3 in the proposed algorithm

are shown in Figures 16–21 that are composed of the restored images and their peak signal-to-noise ratios (PSNRs).

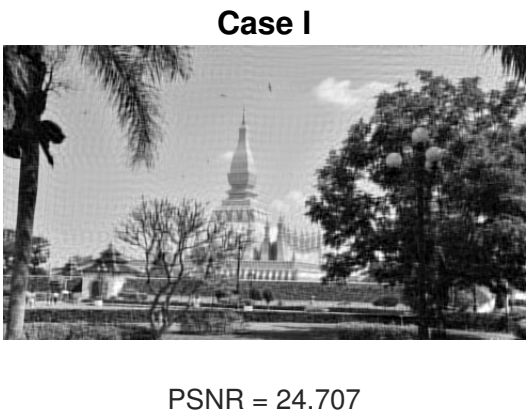

Figure 16. The reconstructed grey image with their PSNRs for three different cases using the proposed algorithm presented in 10,000 iterations, respectively.

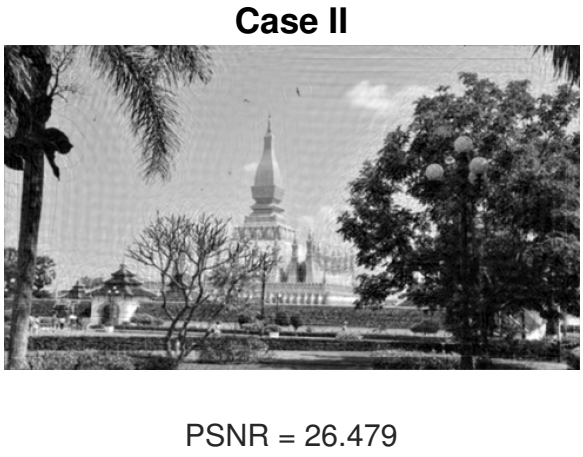

Figure 17. The reconstructed grey image with their PSNRs for three different cases using the proposed algorithm presented in 10,000 iterations, respectively.

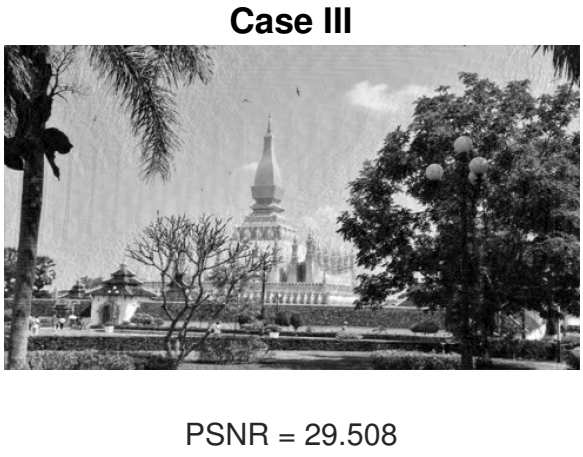

Figure 18. The reconstructed grey image with their PSNRs for three different cases using the proposed algorithm presented in 10,000 iterations, respectively.

Figure 19. The reconstructed RGB image with their PSNRs for three different cases using the proposed algorithm presented in 10,000 iterations, respectively.

Figure 20. The reconstructed RGB image with their PSNRs for three different cases using the proposed algorithm presented in 10,000 iterations, respectively.

Figure 21. The reconstructed RGB image with their PSNRs for three different cases using the proposed algorithm presented in 10,000 iterations, respectively.

Next found the common solutions of a deblurring problem (VIP) with ($N = 2$) by using the proposed algorithm. So, we can consider the results of the proposed algorithm with 10,000 iterations in the following three cases:

Case I: Inputting A_1 and A_2 in the proposed algorithm;
Case II: Inputting A_1 and A_3 in the proposed algorithm; and
Case III: Inputting A_2 and A_3 in the proposed algorithm.

It can be seen from Figures 22–27 that the quality of restored images by using the proposed algorithm in solving the common solutions of the deblurring problem (VIP) with ($N = 2$) was improved compared with the previous results in Figures 16–21 .

Finally, the common solution of the deblurring problem (VIP) with ($N = 3$) using the proposed algorithm was also tested (inputting A_1, A_2, and A_3 in the proposed algorithm).

Figure 22. The reconstructed grey image with their PSNRs for three different cases using the proposed algorithm presented in 10,000 iterations, respectively.

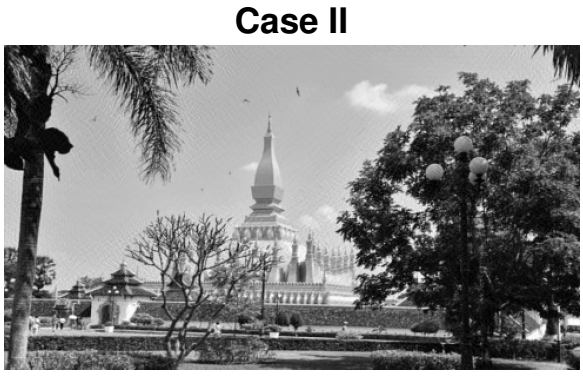

Figure 23. The reconstructed grey image with their PSNRs for three different cases using the proposed algorithm presented in 10,000 iterations, respectively.

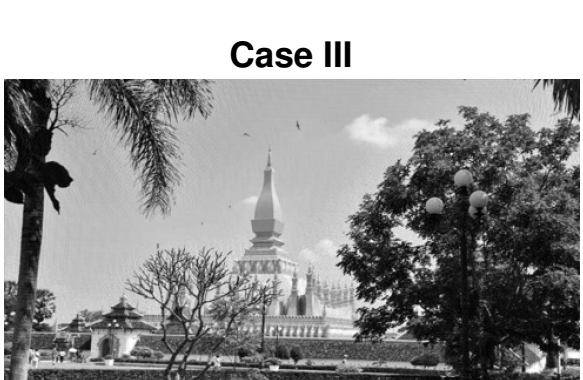

Figure 24. The reconstructed grey image with their PSNRs for three different cases using the proposed algorithm presented in 10,000 iterations, respectively.

Figure 25. The reconstructed RGB image with their PSNRs for three different cases using the proposed algorithm presented in 10,000 iterations, respectively.

Figure 26. The reconstructed RGB image with their PSNRs for three different cases using the proposed algorithm presented in 10,000 iterations, respectively.

Figure 27. The reconstructed RGB image with their PSNRs for three different cases using the proposed algorithm presented in 10,000 iterations, respectively.

Figures 28 and 29 show the reconstructed grey and RGB images with 10,000 iterations. The quality of the recovered grey and RGB images obtained by this algorithm were the highest compared to the previous two algorithms.

PSNR = 34.418

Figure 28. The reconstructed grey image from the blurring operators A_1, A_2, and A_3 using the proposed algorithm presented in 10,000 iterations, respectively.

PSNR = 33.636

Figure 29. The reconstructed RGB image from the blurring operators A_1, A_2, and A_3 using the proposed algorithm presented in 10,000 iterations, respectively.

Moreover, the Cauchy error, the figure error, and the peak signal-to-noise ratio (PSNR) for recovering the degraded grey and RGB images by using the proposed method within the first 10,000 iterations are shown in Figures 30–35.

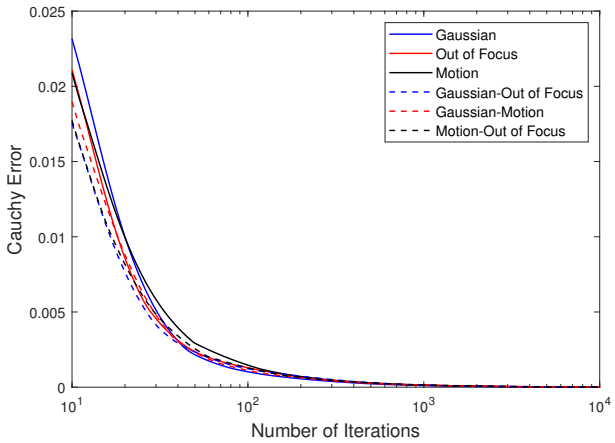

Figure 30. Cauchy error plots of the proposed algorithm in all cases of grey images.

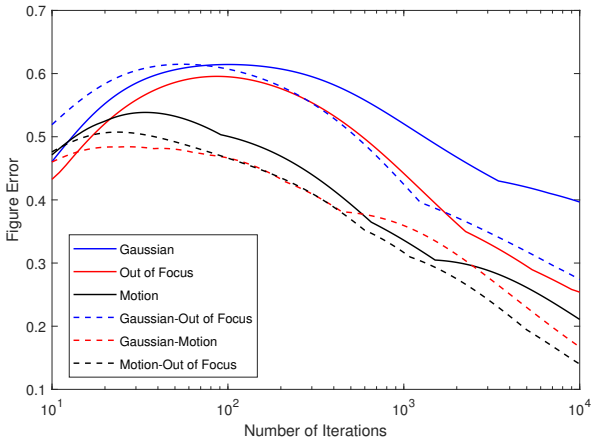

Figure 31. Figure error plots of the proposed algorithm in all cases of grey images.

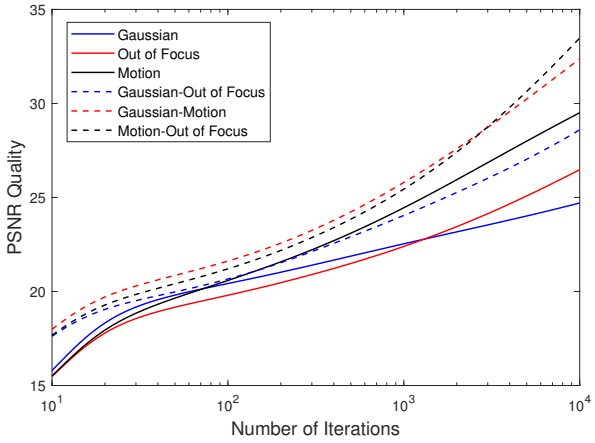

Figure 32. PSNR quality plots of the proposed algorithm in all cases of grey images.

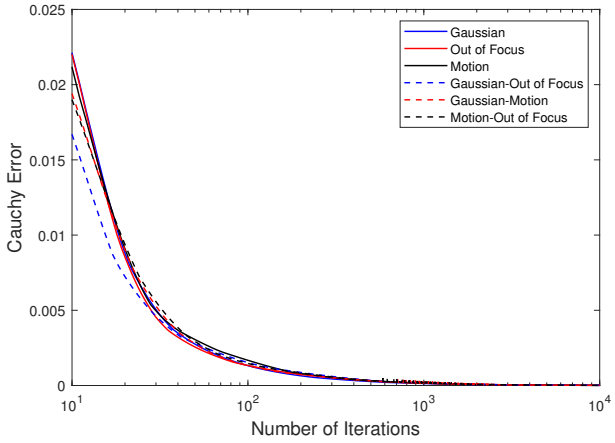

Figure 33. Cauchy error plots of the proposed algorithm in all cases of RGB images.

The Cauchy error is defined as $\|x_n - x_{n-1}\| < 10^{-8}$. The figure error is defined as $\|x_n - x\|$, where x is the solution of the problem (VIP). The performance of the proposed algorithm at x_n in the

image restoration process was measured quantitatively by the means of the peak signal-to-noise ratio (PSNR), which is defined by

$$\mathrm{PSNR}(x_n) = 20\log_{10}\Big(\frac{255^2}{MSE}\Big),$$

where $\mathrm{MSE} = \|x_n - x\|^2$, $\|x_n - x\|$ is the ℓ_2-norm of $\mathrm{vec}(x_n - x)$ and $\mathrm{vec}(x_n - x)$ = A reshape matrix $x_n - x$ as vector.

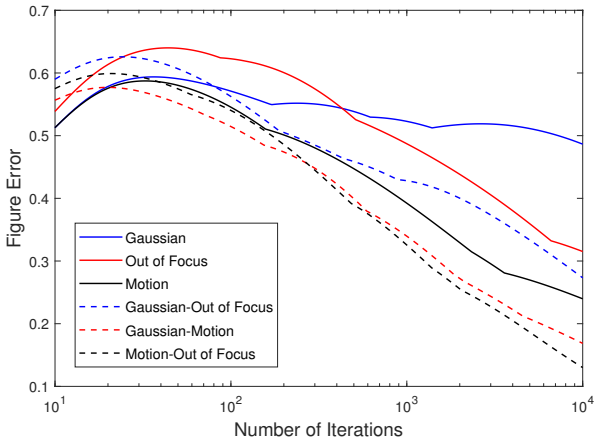

Figure 34. Figure error plots of the proposed algorithm in all cases of RGB images.

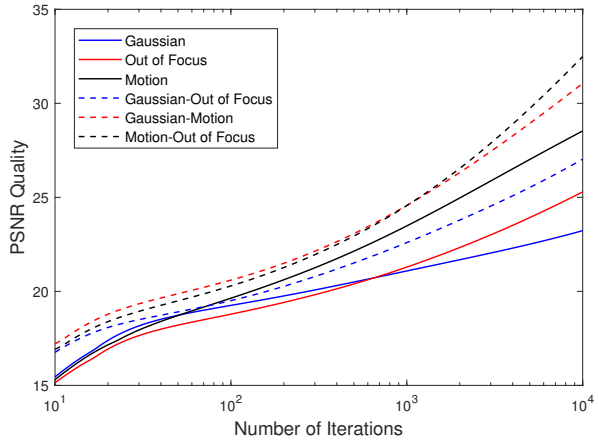

Figure 35. PSNR quality plots of the proposed algorithm in all cases of RGB images.

The Cauchy error plot shows the validity of the proposed method, while the figure error plot confirms the convergence of the proposed method and the PSNR quality plot shows the measured quantitatively of the image. From Figures 30–35, it is clearly seen that the common solution of the deblurring problem (VIP) with $(N \geq 2)$ obtained quality improvements in the reconstructed grey and RGB images. Another advantage of the proposed method when the common solution of two or more image deblurring problems was used to restore the image is that the received image is more consistent than usual (see Figures 36–49). Figures 36–49 show the reconstructed grey and RGB images using the proposed algorithm in obtaining the common solution of the following problem with the same PSNR.

(1) Deblurring problem (VIP) with $(N = 1)$ by inputting A_1, A_2, and A_3 in the proposed algorithm.
(2) Deblurring problem (VIP) with $(N = 2)$ by inputting A_1 and A_2, A_1 and A_3, and A_2 and A_3 in the proposed algorithm respectively.
(3) Deblurring problem (VIP) with $(N = 3)$ by inputting A_1, A_2, and A_3 in the proposed algorithm.

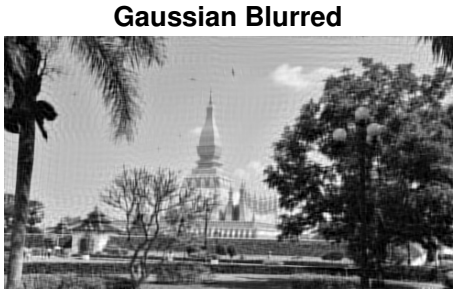

Figure 36. The reconstructed grey image of all cases using the proposed method (2) with PSNR = 24.

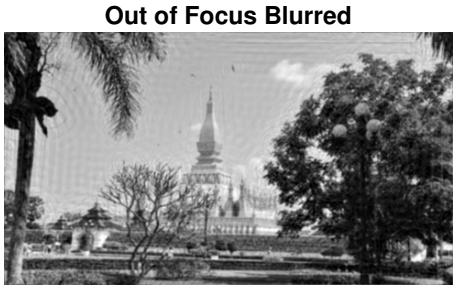

Figure 37. The reconstructed grey image of all cases using the proposed method (2) with PSNR = 24.

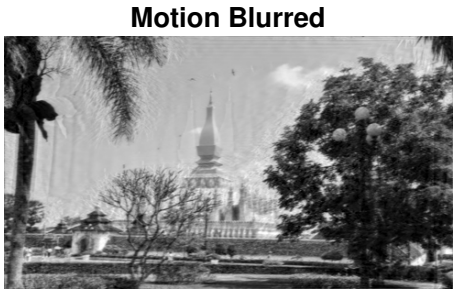

Figure 38. The reconstructed grey image of all cases using the proposed method (2) with PSNR = 24.

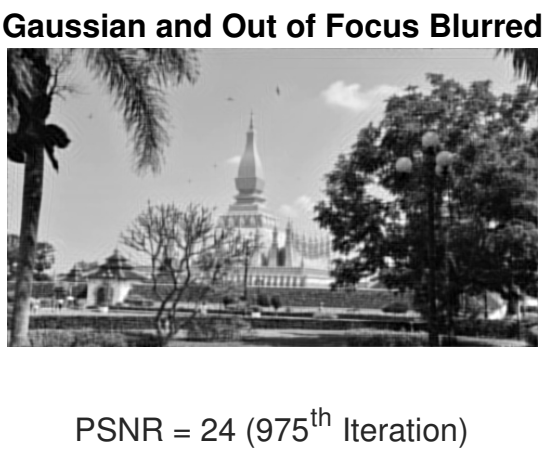

Figure 39. The reconstructed grey image of all cases using the proposed method (2) with PSNR = 24.

Figure 40. The reconstructed grey image of all cases using the proposed method (2) with PSNR = 24.

Figure 41. The reconstructed grey image of all cases using the proposed method (2) with PSNR = 24.

Figure 42. The reconstructed grey image of all cases using the proposed method (2) with PSNR = 24.

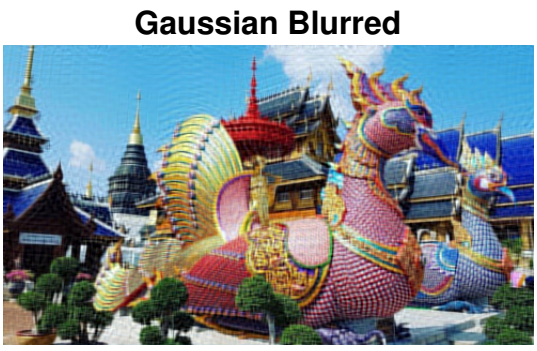

Figure 43. The reconstructed RGB image of all cases using the proposed method (2) with PSNR = 23.

Figure 44. The reconstructed RGB image of all cases using the proposed method (2) with PSNR = 23.

Figure 45. The reconstructed RGB image of all cases using the proposed method (2) with PSNR = 23.

Figure 46. The reconstructed RGB image of all cases using the proposed method (2) with PSNR = 23.

Figure 47. The reconstructed RGB image of all cases using the proposed method (2) with PSNR = 23.

Figure 48. The reconstructed RGB image of all cases using the proposed method (2) with PSNR = 23.

Figure 49. The reconstructed RGB image of all cases using the proposed method (2) with PSNR = 23.

5. Conclusions

In this work, we considered the problem of finding a common solution of variational inequalities with monotonic and Lipschitz operators in a Hilbert space. Under some suitable conditions imposed on the parameters, we proved the strong convergence of the algorithm. Several numerical examples in both finite and infinite dimensional spaces were performed to illustrate the performance of the proposed algorithm (see Tables 1 and 2 and Figures 1–6). We applied our proposed algorithm to image recovery (2) under a situation without knowing the type of matrix blurs to demonstrate the computational performance (see Figures 10–35). We found that the advantage of our proposed algorithm was its ability to restore two or more multiblur effects in an image, giving a restoration performance better than one (see Figures 36–49).

Author Contributions: Supervision, S.S.; formal analysis and writing, P.P. and W.C.; editing and software, D.Y. All authors have read and agreed to the published version of the manuscript.

Funding: This research was funded by Chiang Mai University.

Conflicts of Interest: The authors declare no conflicts of interest.

References

1. Hartman, P.; Stampacchia, G. On some non-linear elliptic diferential-functional equations. *Acta Math.* **1966**, *115*, 271–310. [CrossRef]
2. Aubin, J.-P.; Ekeland, I. *Applied Nonlinear Analysis*; Wiley: New York, NY, USA, 1984.
3. Baiocchi, C.; Capelo, A. *Variational and Quasivariational Inequalities: Applications to Free Boundary Problems*; Wiley: New York , NY, USA, 1984.

4. Glowinski, R.; Lions, J.-L.; Tremolieres, R. *Numerical Analysis of Variational Inequalities*; NorthHolland: Amsterdam, The Netherlands, 1981.
5. Kinderlehrer, D.; Stampacchia, G. *An Introduction to Variational Inequalities and Their Applications*; Academic: New York, NY, USA, 1980.
6. Konnov, I.V. *Combined Relaxation Methods for Variational Inequalities*; Springer: Berlin, Germany, 2001.
7. Nagurney, A. *Network Economics: A Variational Inequality Approach*; Kluwer Academic Publishers: Dordrecht, The Netherlands, 1999.
8. Bauschke, H.H.; Combettes, P.L. *Convex Analysis and Monotone Operator Theory in Hilbert Spaces*; CMS Books in Mathematics; Springer: New York , NY, USA, 2011.
9. Facchinei, F.; Pang, J.-S. *Finite-Dimensional Variational Inequalities And Complementarity Problems*; Springer Series in Operations Research; Springer: New York, NY, USA, 2003; Volume II.
10. Cholamjiak, P.; Suantai, S.Viscosity approximation methods for a nonexpansive semigroup in Banach spaces with gauge functions. *J. Glob. Optim.* **2012**, *54*, 185–197. [CrossRef]
11. Shehu, Y.; Cholamjiak, P. Iterative method with inertial for variational inequalities in Hilbert spaces. *Calcolo* **2019**. [CrossRef]
12. Kesornprom, S.; Cholamjiak, P. Proximal type algorithms involving linesearch and inertial technique for split variational inclusion problem in hilbert spaces with applications. *Optimization* **2019**, *68*, 2365–2391. [CrossRef]
13. Cholamjiak, P.; Thong, D.V.; Cho, Y.J. A novel inertial projection and contraction method for solving pseudomonotone variational inequality problems. *Acta Appl. Math.* **2019**. [CrossRef]
14. Anh, P.N.; Hien, N.D.; Phuong, N.X. A parallel subgradient method extended to variational inequalities involving nonexpansive mappings. *Appl. Anal.* **2018**. [CrossRef]
15. Ceng, L.C.; Coroian, I.; Qin, X.; Yao, J.C. A general viscosity implicit iterative algorithm for split variational inclusions with hierarchical variational inequality constraints. *Fixed Point Theory* **2019**, *20*, 469–482. [CrossRef]
16. Korpelevich, G.M. The extragradient method for finding saddle points and other problems. *Ekonomikai Matematicheskie Metody* **1976**, *12*, 747–756.
17. Censor, Y.; Gibali, A.; Reich, S. The subgradient extragradient method for solving variational inequalities in Hilbert space. *J. Optim. Theory Appl.* **2011**, *148*, 318–335. [CrossRef]
18. Gibali, A. A new non-Lipschitzian projection method for solving variational inequalities in Euclidean spaces. *J. Nonlinear Anal. Optim.* **2015**, *6*, 41–51.
19. Shehu, Y.; Iyiola, O.S. Strong convergence result for monotone variational inequalities. *Numer. Algorithms* **2016**. [CrossRef]
20. Censor, Y.; Gibali, A.; Reich, S.; Sabach, S. Common solutions to variational inequalities. *Set Val. Var. Anal.* **2012**, *20*, 229–247. [CrossRef]
21. Bauschke, H.H., Borwein, J.M. On projection algorithms for solving convex feasibility problems. *SIAMRev* **1996**, *38*, 367–426. [CrossRef]
22. Stark, H. (Ed.) *Image Recovery Theory and Applications*; Academic: Orlando, FL, USA, 1987.
23. Censor, Y.; Chen, W.; Combettes, P.L.; Davidi, R.; Herman, G.T. On the effectiveness of projection methods for convex feasibility problems with linear inequality constraints. *Comput. Optim. Appl.* **2011**. [CrossRef]
24. Hieu, D.V.; Anh, P.K.; Muu, L.D. Modified hybrid projection methods for finding common solutions to variational inequality problems. *Comput. Optim. Appl.* **2016**. [CrossRef]
25. Hieu, D.V. Parallel hybrid methods for generalized equilibrium problems and asymptotically strictly pseudocontractive mappings. *J. Appl. Math. Comput.* **2016**. [CrossRef]
26. Yamada, I. The hybrid steepest descent method for the variational inequality problem over the intersection of fixed point sets of nonexpansive mappings. In *Inherently Parallel Algorithms in Feasibility and Optimization and Their Applications*; Butnariu, D., Censor, Y., Reich, S., Eds.; Elsevier: Amsterdam, The Netherlands, 2001; pp. 473–504.
27. Yao, Y.; Liou, Y.C. Weak and strong convergence of Krasnoselski-Mann iteration for hierarchical fixed point problems. *Inverse Probl.* **2008**, *24*, 015015. [CrossRef]
28. Anh, P.K.; Hieu, D.V. Parallel and sequential hybrid methods for a finite family of asymptotically quasi ϕ-nonexpansive mappings. *J. Appl. Math. Comput.* **2015**, *48*, 241–263. [CrossRef]
29. Anh, P.K.; Hieu, D.V. Parallel hybrid methods for variational inequalities, equilibrium problems and common fixed point problems. *Vietnam J. Math.* **2015**. [CrossRef]

30. Takahashi, W. *Nonlinear Functional Analysis*; Yokohama Publishers: Yokohama, Japan, 2000.
31. Xu, H.-K. Iterative algorithms for nonlinear operators. *J. Lond. Math. Soc.* **2002**, *66*, 240–256. [CrossRef]
32. Takahashi, S.; Takahashi, W. Strong convergence theorem for a generalized equilibrium problem and a nonexpansive mapping in a Hilbert space. *Nonlinear Anal.* **2008**, *69*, 1025–1033. [CrossRef]
33. Engl, H.W.; Hanke, M.; Neubauer, A. *Regularization of Inverse Problems*; Kluwer Academic Publishers: Dordrecht, The Netherlands, 2000.
34. Hansen, P.C. *Rank-Deficient and Discrete Ill-Posed Problems*; SIAM: Philadelphia, PA, USA, 1997.
35. Hansen, P.C. *Discrete Inverse Problems: Insight and Algorithms*; SIAM: Philadelphia, PA, USA, 2010.
36. Vogel, C.R. *Computational Methods for Inverse Problems*; SIAM: Philadelphia, PA, USA, 2002.